geotechnics

MDPI

Article

Evaluation of Shear Wave Velocity Prediction Models from Standard Penetration Test N Values Depending on Geologic Attributes: A Case Study in Busan, South Korea

Giseok Heo [1], Jaehwi Kim [2], Seokho Jeong [2] and Dongyoup Kwak [1,*]

[1] Department of Civil and Environmental Engineering, Hanyang University, ERICA, 55 Hanyangdaehak-ro, Sangnok-gu, Ansan 15588, Gyeonggi-do, Republic of Korea; gsheo@hanyang.ac.kr
[2] Department of Civil Engineering, Changwon National University, 20 Changwondaehak-ro, Uichang-gu, Changwon 51140, Gyeongsangnam-do, Republic of Korea; 20143041@changwon.ac.kr (J.K.); seokho.jeong@changwon.ac.kr (S.J.)
* Correspondence: dkwak@hanyang.ac.kr; Tel.: +82-31-400-5141

Abstract: This study evaluates the effectiveness of the previously proposed Standard Penetration Test (SPT) N and shear wave velocity (V_S) models in relation to the geological attributes of the Busan region, situated in the southeastern part of the Korean peninsula. The multiple empirical N-V_S models, which used datasets collected from different regions in South Korea, resulted in distinct N-V_S trends across models. To validate the predictive capabilities of each model, this study gathered boring logs containing SPT N and V_S measurements within the Busan region, followed by a thorough residual analysis. The Busan area encompasses a delta region to the west and erosion basins within the mountains and hills to the east. Despite the relatively confined geographical scope, we found that models developed using data from fill areas exhibit superior performance for the delta region (western Busan), while models constructed from datasets within erosion basins perform better for the erosion basin region (eastern Busan). This comparative examination supports the dependence of the N-V_S model on geologic attributes and offers the valuable insight that N-V_S models developed with analogous geological attributes should be employed when estimating V_S from SPT N values.

Keywords: SPT N; shear wave velocity; N-V_S model; delta; erosion basin

check for updates

Citation: Heo, G.; Kim, J.; Jeong, S.; Kwak, D. Evaluation of Shear Wave Velocity Prediction Models from Standard Penetration Test N Values Depending on Geologic Attributes: A Case Study in Busan, South Korea. *Geotechnics* **2023**, *3*, 1004–1016. https://doi.org/10.3390/geotechnics3040054

Received: 28 August 2023
Revised: 22 September 2023
Accepted: 28 September 2023
Published: 1 October 2023

Copyright: © 2023 by the authors. Licensee MDPI, Basel, Switzerland. This article is an open access article distributed under the terms and conditions of the Creative Commons Attribution (CC BY) license (https://creativecommons.org/licenses/by/4.0/).

1. Introduction

Shear wave velocity (V_S) can be directly measured in the field through geophysical investigation such as downhole, crosshole, SASW (Spectral Analysis of Surface Waves), and MASW (Multi-Channel Analysis of Surface Waves) tests. However, in South Korea, the direct measurement of V_S using these geophysical investigations was not commonly conducted before significant earthquakes like 2016 M_L 5.8 Gyeongju earthquake and 2017 M_L 5.4 Pohang earthquake. The primary approach for site investigation has been Standard Penetration Tests (SPTs), which are a fundamental geotechnical investigation technique utilized for soil sampling and assessing subsurface conditions. SPT results are often accessible within the geotechnical investigation database for sites where construction projects were performed.

Leveraging the extensive dataset generated by SPT, various studies have proposed N-V_S models for the prediction of V_S [1–10]. Imai and Yoshimura [5] were the pioneers in establishing the N-V_S relationships in Japan. Since then, multiple research endeavors have sought to refine and enhance the accuracy of these N-V_S relationships. Certain investigations have refined the N to N_{60}, representing 60% of the energy efficiency of the hammer blow [1,11–14]. Some studies have incorporated the $(N_1)_{60}$, integrating corrections for confining pressure [10,15]. Furthermore, specific studies have supported the N with additional parameters, such as depth or vertical effective stress, to further improve the precision of V_S predictions [1,3,16].

N-V_S models suggested previously are dependent on soil type, layer composition, and geological attributes. Rahim et al. [17] established N-V_S relationships based on geological age, and Rao and Choudhury [9] proposed N-V_S relationships tailored for the northwestern part of Haryana, India, specifically for sedimentary layers with a thickness of 230–340 m. Piratheepan [18] conducted a comparative study evaluating the effectiveness of N-V_S relationships by analyzing depositional layers using data from accumulative sedimentary layers in the United States, Canada, and Japan. Ohta and Goto [8] proposed N-V_S relationships grouped in geological age (Pleistocene and Holocene), and Ohsaki and Iwasaki [7] proposed N-V_S relationships tailored to sedimentary layers formed through accumulative, fluvial Pliocene deposits across 200 regions in Japan. Imai and Tonouchi [4] proposed an N-V_S relationship using 1600 boring logs across Japan, and Kwak et al. [16] developed N-Vs relationships contingent upon soil types using data from 1102 boring logs from the Kyoshin network (K-NET) seismic observation stations.

On the other hand, there are also studies that N-V_S relationships are independent from soil type. Hasancebi and Ulusay [12] and Dikmen [19] proposed N-V_S models that remain insensitive to soil type. Their comprehensive analysis across various soil layers concluded that the influence of soil type on N-V_S relationships is negligible.

Within South Korea, Kim [6] gathered data from Yeongjong Island in Incheon, revealing a sedimentary layer of roughly 52 m in thickness superimposed over bedrock, complemented by an additional reclamation layer measuring approximately 7.5 m. Focusing on sedimentary layers of approximately 25 m thickness topped by a 10 m reclamation layer in the Saemangeum reclamation area, Chae [1] proposed the N-V_S relationship while considering the energy efficiency of V_S and N values. Sun et al. [10] suggested N-V_S models through V_S measurements acquired via crosshole, downhole, and uphole techniques, utilizing data from 26 boreholes situated across eight distinct regions. Do et al. [2] established N-V_S empirical equations employing V_S data acquired from suspension PS logging (SPS) tests performed in 19 boreholes within the Chungcheong-do region. Heo and Kwak [3] proposed N-V_S models based on a comprehensive dataset obtained from 577 boreholes spanning the entire country. The geographical distribution of datasets employed for model development in each of these studies is depicted in Figure 1.

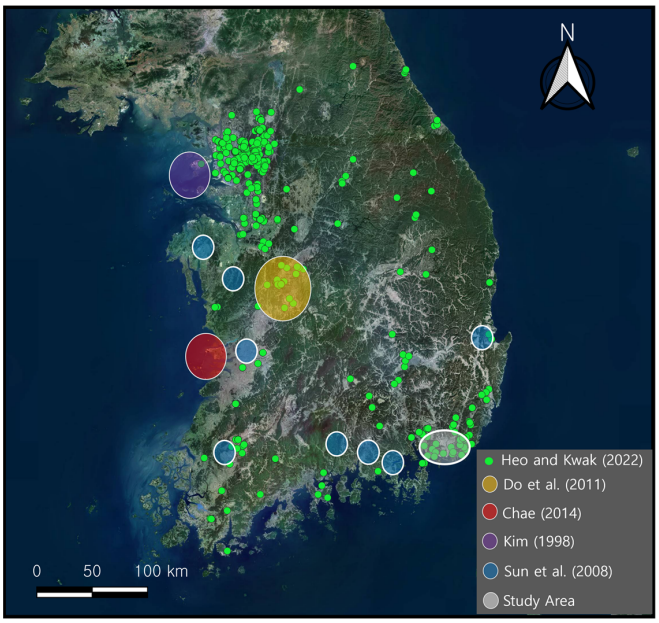


Figure 1. Location of dataset used for model development for each model [1–3,6,10].

Table 1 provides an overview of previously proposed N-V_S relationships, while Figure 2 shows N-V_S relationships for all soil types grouped by country. Even though originating from diverse reclamation locations in South Korea, the N-Vs relationships intro-

duced by Kim [6] and Chae [1] exhibit similar trends. Comparing them to international models, the N-V_S relationships proposed for the reclamation area in South Korea [1,6] have similar trends with those proposed in Japan [4,5,7,8] and India [9], where sedimentary layer thickness ranges from 230 to 340 m. Conversely, in cases such as Do et al. [2] and Heo and Kwak [3], where a predominant proportion of the dataset is from erosion basins that are a common geological attribute of urbanized areas in South Korea, higher V_S values for identical N values are anticipated compared to N-V_S relationships derived from reclamation areas. The model outlined by Sun et al. [10] displays a distinct trend. It has the lowest V_S at a low N-value (<10) and the highest V_S at a stiff layer (N > 200) among Korean models. It may be attributed to the fact that the study locations of Sun et al. [10] are at a loose and deep stratum for a low N-value range.

Table 1. N-V_S models of previous studies for each country.

Country	Study	N-V_S (m/s) Model *	Type	R^2
Japan	Imai and Yoshimura [5]	$V_S = 76N^{0.33}$	All soil	-
	Ohsaki and Iwasaki [7]	$V_S = 81.4N^{0.39}$	All soil	0.89
		$V_S = 59.4N^{0.47}$	Sand	-
	Ohta and Goto [8]	$V_S = 85.35N^{0.348}$	All soil (Pleistoene)	0.72
		$V_S = 92.2N^{0.27}$	All soil (Holocene)	-
		$V_S = 88.4N^{0.333}$	Sand (Pleistoene)	-
		$V_S = 86.9N^{0.333}$	Clay (Pleistoene)	-
	Imai and Tonouchi [4]	$V_S = 97N^{0.314}$	All soil	0.87
		$V_S = 87.8N^{0.314}$	Sand	0.69
		$V_S = 107N^{0.274}$	Clay	0.72
Korea	Sun et al. [10]	$V_S = 65.64N^{0.407}$	All soil	0.56
		$V_S = 82.01N^{0.319}$	Sand and Silt	0.34
		$V_S = 78.63N^{0.361}$	Gravel	0.33
		$V_S = 75.76N^{0.371}$	Weathered soil	0.25
		$V_S = 107.94N^{0.418}$	Weathered rock	0.22
	Do et al. [2]	$V_S = 125.3N^{0.26}$	All soil	0.70
		$V_S = 111.7N^{0.32}$	Sand	0.65
		$V_S = 117.6N^{0.28}$	Clay	0.49
		$V_S = 111.1N^{0.27}$	Gravel	0.59
		$V_S = 176.5N^{0.17}$	Weathered soil	0.29
		$V_S = 215.5N^{0.18}$	Weathered rock	0.25
	Heo and Kwak [3]	$V_S = 140.3N^{0.2529}$	All soil	0.72
		$V_S = 129.5N^{0.22}D^{0.098}$	All soil	0.73
		$V_S = 159.2N^{0.1706}$	Sand	0.17
		$V_S = 140.5N^{0.2142}$	Clay and Silt	0.18
		$V_S = 153.2N^{0.201}$	Gravel	0.23
		$V_S = 151N^{0.2363}$	Weathered soil	0.32
		$V_S = 313.8N^{0.1149}$	Weathered rock	0.06
	Chae [1]	$V_S = 109.7N^{0.25}$	All soil	0.69
		$V_S = 75.5N^{0.176}D^{0.196}$	All soil	0.83
		$V_S = 85.5N^{0.31}$	Sand	0.77
		$V_S = 132.4N^{0.187}$	Clay and Silt	0.41
	Kim [6]	$V_S = 98.38N^{0.29}$	All soil	-
India	Rao and Choudhury [9]	$V_S = 84N^{0.38}$	All soil	0.90

* N: SPT N-value; D: depth in meter unit.

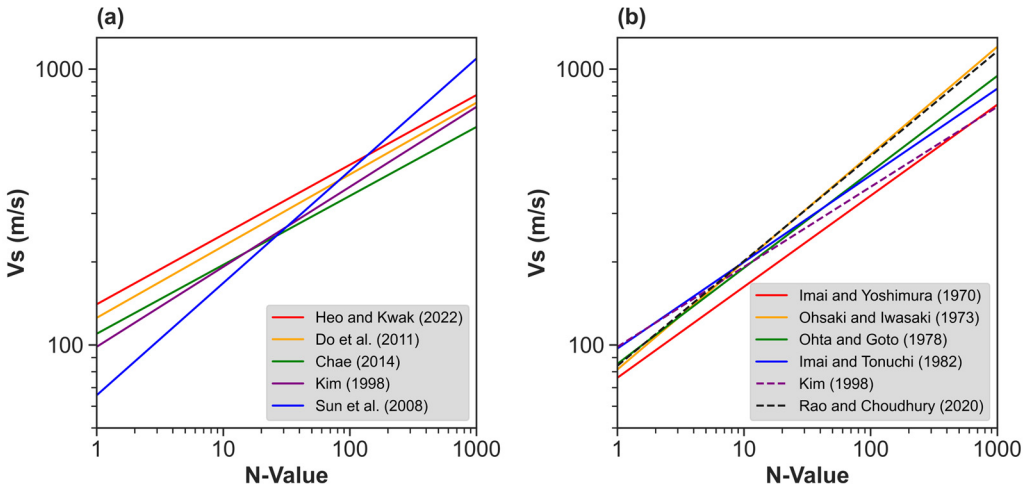


Figure 2. N-V_S models proposed in different countries: (**a**) South Korea and (**b**) other countries [1–10].

As indicated above, N-V_S relationships exhibit consistent trends when the geological attributes of the originating datasets are comparable. Conversely, distinct trends are shown if geological attributes differ.

This study evaluates the prediction performance of N-V_S models suggested in South Korea through residual analyses, using datasets acquired from the Busan region. The Busan area encompasses disparate geological regions: a delta region to the west and erosion basins to the east. Based on the evaluation, a guideline is established for the enhanced prediction of V_S from N values, aligning with the diverse geological features of the study area.

2. Study Area and Dataset

2.1. Study Area

The Busan region is located in the southeastern part of the Korean peninsula. It features distinct geological attributes, with the Nakdonggang delta area situated to the west of Busan and the eastern part of the Busan marked by erosion basins that are surrounded by mountains and hills. This geographic division is illustrated in Figure 3.

The Nakdonggang delta is located downstream of the Nakdonggang River in South Korea. This region has undergone the accumulation of substantial sediment layers due to fluctuations in sea levels [20,21]. It holds the distinction of being the largest delta area on the Korean peninsula. A study conducted by Lee et al. [22] covered a span from 1984 to 2015, investigating the changes of sedimentation in the terrain of the Nakdonggang River estuary over a 31-year period. The changes of sediment thickness are attributed to a combination of natural factors such as sea level rise, tides, and seismic activity, as well as human interventions including the construction of artificial structures like harbors and alterations to waterways.

The eastern part of Busan features erosion basins surrounded by mountains and hills, which is a common geological formation in urban areas of South Korea [23–26]. These erosion basins typically have mountainous perimeters and lower-lying central areas, formed through processes like differential weathering and erosion. Within these basins, alluvial fans often form due to the accumulation of weathered layers and the presence of small streams [24,25]. However, the thickness of sediment layers in these alluvial fans is generally not as substantial as in other alluvial fan regions, leading to the classification of these areas as pediments rather than traditional alluvial fans [27]. The distinction between pediments and alluvial fans based on sediment thickness has been a topic of global discussion [28], and recent studies have undertaken comparisons between Korean alluvial fans and those in other countries [29,30].

In Japan, in contrast, mountainous watersheds play a significant role in generating substantial sediment production. Particularly in areas with steep terrain, the annual sediment production can exceed 1000 m^3/km^2, and in certain cases, it can even reach over 10,000 m^3/km^2. These values are comparable to the highest levels of sediment production recorded in mountainous watersheds worldwide and are much higher than those observed in most other mountainous regions globally. As a consequence of this abundant sediment supply, alluvial fans are widely distributed along the fronts of mountains in Japan [31,32]. These geological differences between South Korea and Japan can lead to variations in N-V_S relationships, as illustrated in Figure 2.

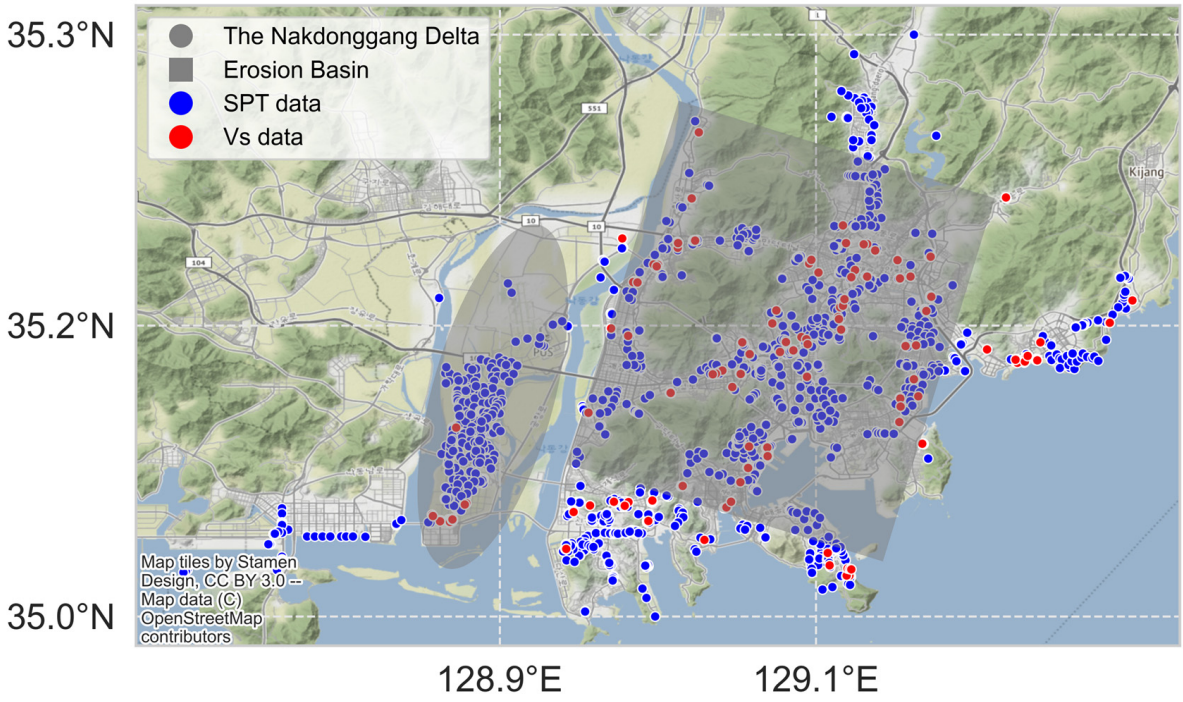


Figure 3. Regions of the Nakdonggang delta and erosion basin and locations of boring log data in Busan.

2.2. Dataset

Figure 3 shows the borehole locations where borehole profiles have been collected from the South Korean geotechnical database, GeoInfo (National Geotechnical Information Center). GeoInfo serves as a repository for ground investigations conducted at construction sites across South Korea [33]. The borehole records were excluded following the filtering criteria suggested in Heo and Kwak [3]. As a result, a total of 1794 borehole records remained for analysis containing SPT data and stratigraphic information. Additionally, the dataset includes 123 borehole records with measurements of V_S obtained through downhole tests. Using the compiled dataset, various geotechnical attributes are determined. Specifically, the thickness of sedimentary layers, defined as the alluvial soil layer, and the depth to the underlying bedrock, defined as the soft rock or stiffer layer, are calculated. It is important to note that the thickness of sedimentary layers and the depth to the bedrock are distinct attributes. Soil layers within the profiles typically include fill, alluvial soil (AS), weathered soil (WS), and weathered rock (WR), extending from the surface to the bedrock. The bedrock depth is calculated by adding up the thicknesses of all soil layers, whereas the sedimentary layer thickness specifically refers to the thickness of the alluvial soil layer.

The distribution of the depth to the bedrock and sedimentary layer thickness across the study area is illustrated in Figure 4. In the Nakdonggang delta, there is a widespread occurrence of sites with sedimentary layers exceeding 70 m in thickness. However, it is notable that there is a lack of measurements for bedrock depth in this region. This suggests

that there are numerous boreholes that do not reach the bedrock layer. The bedrock depth in the Nakdonggang delta area is known to range from 20 to 90 m [34]. On the contrary, the erosion basins located in the eastern part of Busan exhibit sedimentary layers that are approximately 10 m thick, with bedrock depths ranging within 30 m.

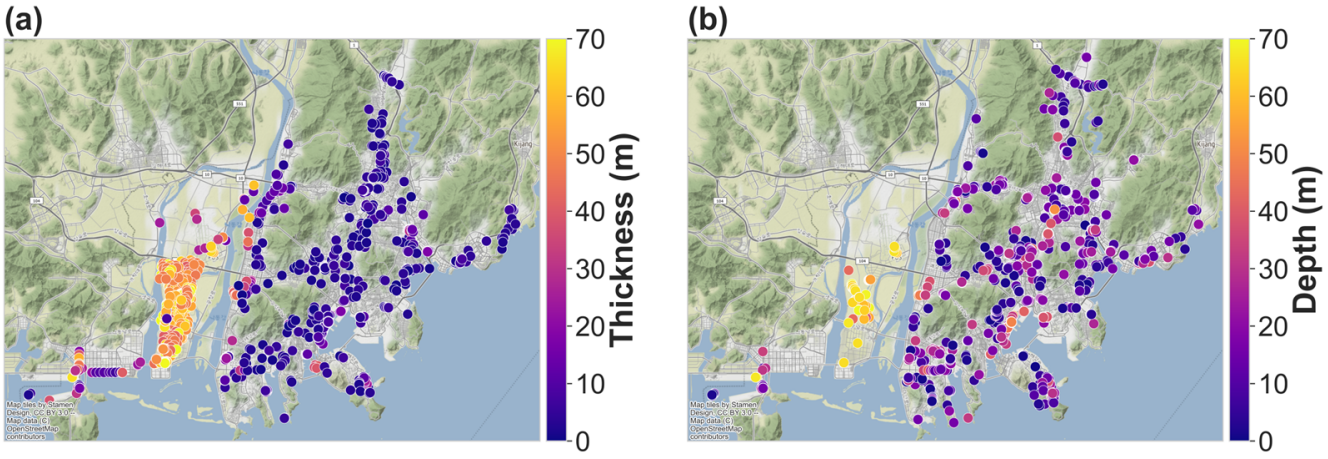


Figure 4. (**a**) Thickness of sedimentary layers and (**b**) depth to the bedrock of boreholes in the Busan region.

Table 2 provides quartile values representing the depth of each soil layer in both the Nakdonggang delta and the erosion basins. While the median thickness of the landfill layer (Fill) is relatively similar between the delta (1.4 m) and the erosion basin (2.3 m), the median thickness of sedimentary layers (AS) differs significantly. In the delta region, sedimentary layers have a median thickness value of approximately 58 m, whereas in the erosion basin, the value is approximately 5 m. This results in a substantial difference of about 12 times in the sedimentary layer thickness between these two terrains. The weathered soil layer thickness also differs between the delta and the erosion basin. In the delta, this layer has a medium thickness of 2 m, whereas in the erosion basin, it is approximately 7 m. Despite the shallower depth, the erosion basin exhibits a thicker weathered soil layer than the delta region. On the other hand, the medium thickness of the weathered rock layer is similar, where both regions have 6 m of thickness.

Table 2. Quantile of depth for each type of layer depending on regions.

	Delta				**Erosion Basin**			
		Top–Bot (m)				**Top–Bot (m)**		
Layer	**Count**	**25%**	**50%**	**75%**	**Count**	**25%**	**50%**	**75%**
Fill	435	0.0–0.8	0.0–1.4	0.0–3.5	1449	0.0–1.5	0.0–2.3	0.0–4.0
AS	471	0.7–49	1.2–59	2.8–65	726	1.5–5.0	2.4–7.5	4.0–15
WS	46	27–31	65–67	67–70	1154	2.0–6.5	4.2–11	8.0–18
WR	115	59–65	67–73	73–81	1077	6.5–10	12–18	19–28

Figure 5 visually represents the distribution of N values and V_S measurements obtained for both the Nakdonggang delta (indicated by red points) and the erosion basin terrains (indicated by blue points). It is evident that the delta region tends to have lower V_S values compared to the erosion basin terrain for the same N values. This disparity in V_S values based on N values is important because it highlights the geological influence on the N-V_S relationship. As a consequence, when dealing with the Nakdonggang delta terrain, utilizing N-V_S relationships that are derived from terrains resembling erosion basins could potentially lead to an overestimation of V_S values [3]. Conversely, applying

N-V_S relationships formulated for delta-like terrains to the erosion basin terrain might result in an underestimation of V_S values [6]. This finding emphasizes the need to consider the geological context and terrain characteristics when selecting appropriate N-V_S relationships for different regions to ensure accurate predictions of V_S. This study further emphasizes the use of proper N-V_S relationships when predicting V_S from N in analyzing the time-averaged V_S of soil layers in subsequent sections.

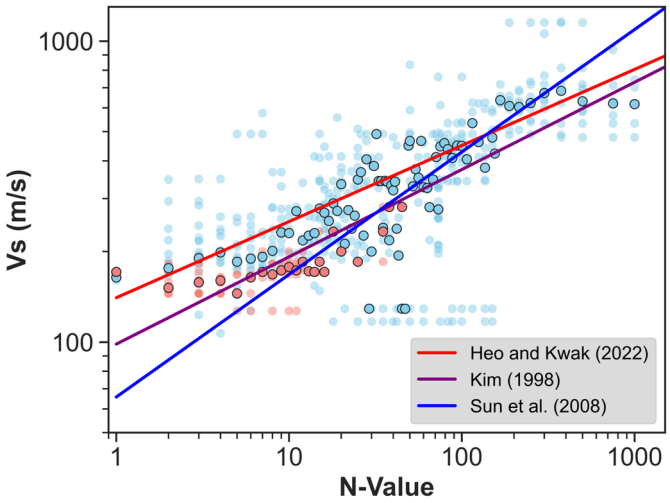


Figure 5. Relationship between N value and V_S. Blue dots indicate sites at erosion basins and red dots indicate sites at the delta region. Regression models [3,6,10] are overlapped.

3. Methodology

Among the collected dataset, there are V_S measurements as well as SPT N measurements at 123 boreholes. The primary evaluation metric used in this study to assess the effectiveness of N-V_S models depending on geological attribute is the time-averaged V_S of soil layers ($V_{s,soil}$). The choice of $V_{s,soil}$ as the primary evaluation metric is justified by its ability to provide a comprehensive representation of the potential N-V_S relationship bias at a specific site. $V_{s,soil}$ serves as a valuable single value that captures the cumulative impact of any potential bias in the N-V_S relationship for a particular location. By utilizing $V_{s,soil}$ as the evaluation metric, the study aims to gauge how well the N-V_S models account for the geological attributes specific to each terrain type in the Busan region. This approach allows for a more comprehensive understanding of the model's effectiveness in predicting V_S under varying geological conditions.

To calculate $V_{s,soil}$, both the thickness of soil layers and their corresponding V_S down to the bedrock depth are required. However, if the depth of the borehole does not extend to the bedrock level, determining the thickness of the soil layers becomes challenging, preventing the calculation of $V_{s,soil}$. In such cases, an alternative metric, V_{s30}, is computed and utilized for validation. The calculation of $V_{s,soil}$ is performed as follows:

$$V_{s,soil} = \frac{\sum_i^n h_i}{\sum_i^n \frac{h_i}{V_{s,i}}} \quad (1)$$

where h_i and $V_{s,i}$ are the thickness and V_S of the ith layer, respectively, and n indicates the number of soil layers. The V_{s30} can be calculated as follows:

$$V_{s30} = \frac{\sum_i^{n_{30}} h_i}{\sum_i^{n_{30}} \frac{h_i}{V_{s,i}}} \quad (2)$$

where n_{30} refers to the number of layers down to the 30 m depth.

If V_S measurements are available for a site, both $V_{s,soil}$ and V_{s30} can be directly calculated. However, in cases where V_S measurements are not available, V_S must be estimated using SPT N values through N-V_S relationships. Using the N-V_S models proposed by Kim [6] (K98), Sun et al. [10] (SEA08), and Heo and Kwak [3] (HK22), calculations were performed to determine either $V_{s,soil}$ or V_{s30}. To avoid overestimating V_S, the threshold N values suggested by Heo and Kwak [3] for each soil layer type were employed during the calculations, regardless of N-V_S models.

Boring logs were excluded from residual analysis described in the subsequent section if they met the following criteria:

- The depth of the borehole was shallower than both the bedrock depth and 30 m;
- SPT measurements were conducted with intervals greater than 5 m;
- Neither SPT nor V_S measurements were available down to a depth of 30 m.

Consequently, a total of 82 boreholes with calculated $V_{s,soil}$ or V_{s30} using field-measured V_S and 770 boreholes using N-Vs relationships were retained for residual analysis.

Figure 6 illustrates the distribution of $V_{s,soil}$ or V_{s30} values across different boreholes. In the Nakdonggang delta region, the range of $V_{s,soil}$ spans approximately 150 to 250 m/s, while in the erosion basin area, the distribution is predominantly above 300 m/s. Specifically, Figure 6a displays the $V_{s,soil}$ values obtained from field-measured V_S data, while Figure 6b–d present $V_{s,soil}$ values calculated from the N-V_S models of HK22, SEA08, and K98, respectively. Within the Nakdonggang delta region, the $V_{s,soil}$ distributions from the K98 and SEA08 models closely align with the field-measured $V_{s,soil}$ distribution, falling around 100 to 200 m/s. In contrast, the HK22 model exhibits a higher distribution ranging from 200 to 300 m/s. Conversely, in the erosion basin areas surrounded by mountains and hills, the HK22 model's $V_{s,soil}$ distribution surpasses 300 m/s, consistent with the distribution of field-measured $V_{s,soil}$. In this region, the K98 and SEA08 models show distributions primarily between 200 to 300 m/s. These observations highlight the variations in predicted $V_{s,soil}$ values across different N-V_S models and terrains, emphasizing the importance of geological attributes in influencing the model's performance and accuracy.

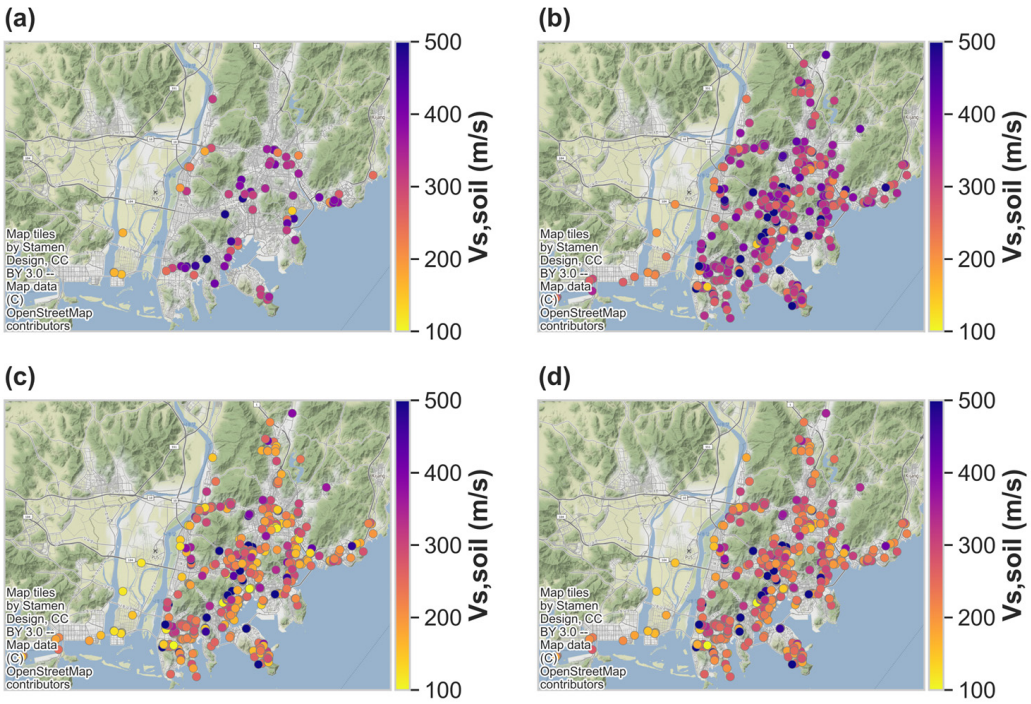


Figure 6. Distribution of $V_{s,soil}$ at boreholes in Busan region calculated using various ways: (**a**) direct V_S measurements, (**b**) V_S predicted using HK22, (**c**) V_S predicted using SEA08, and (**d**) V_S predicted using K98.

4. Result and Discussions

For the purpose of residual analysis, the $V_{s,soil}$ obtained from measured V_S profiles were utilized as the reference. Residuals were calculated as the discrepancy between the log-normal-transformed measured $V_{s,soil}$ and the predicted log-normal $V_{s,soil}$ values from each of the three N-V_S models [3,6,10]. The log-normal transformation was employed due to the log-normal distribution typically observed in the $V_{s,soil}$ data. The evaluation of the three models' performances in both the delta and erosion basin regions involved determining the mean (μ) and standard deviation (σ_{ln}) of the residuals for each geological attribute within these regions. Figure 7 visually represents the spatial distribution and probability density function of these residuals, while Table 3 offers a summarized account of the μ and σ_{ln} values associated with each model and region.

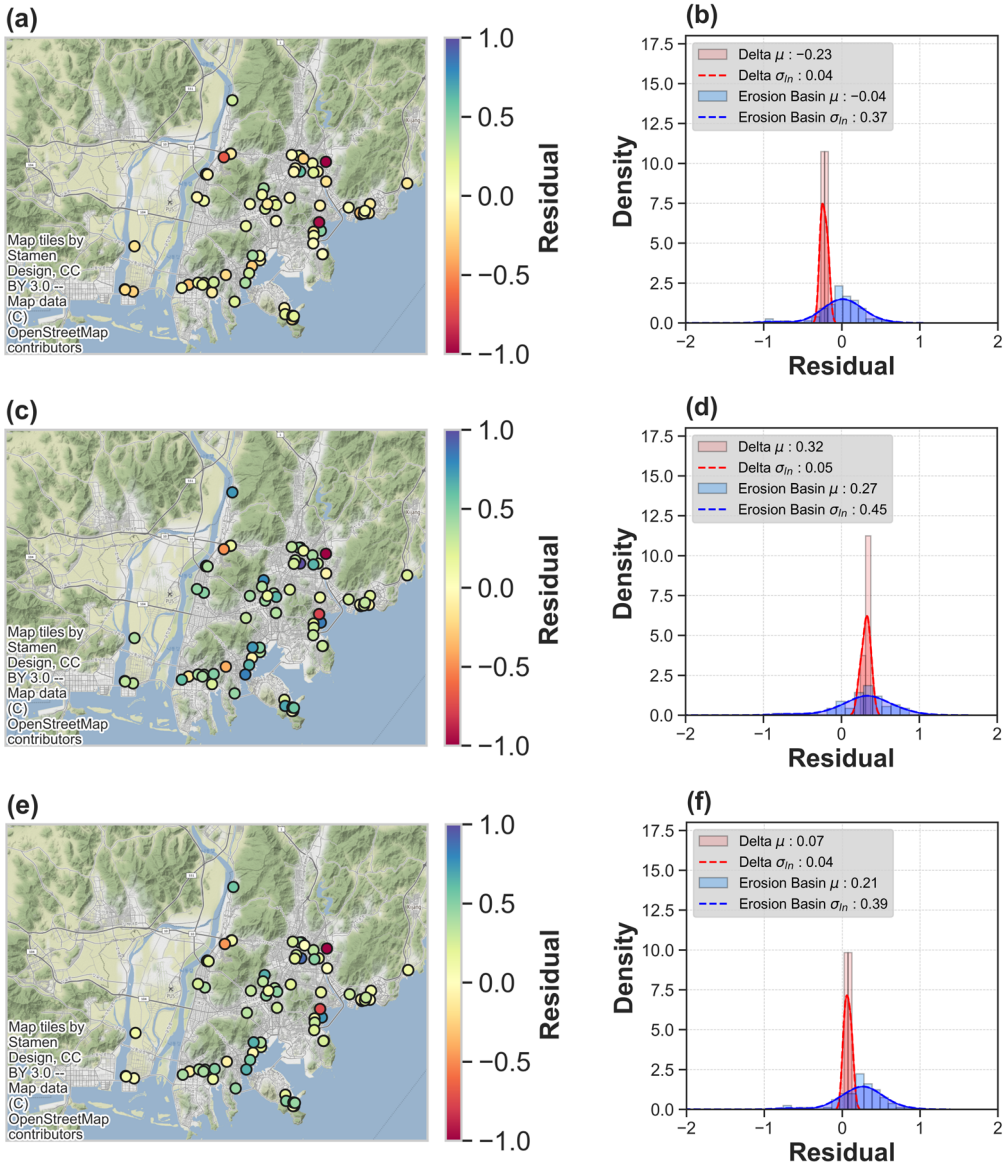


Figure 7. Spatial distribution of $V_{s,soil}$ residuals using (**a**) HK22, (**c**) SEA08, and (**e**) K98 and population density at the delta region (red) and erosion basin regions (blue) using (**b**) HK22, (**d**) SEA08, and (**f**) K98.

Table 3. Mean and standard deviation of residuals.

Region	Model	Mean (μ)	Standard Deviation (σ_{ln})
Delta	Heo and Kwak [3] (HK22)	−0.23	0.04
	Sun et al. [10] (SEA08)	0.32	0.05
	Kim [6] (K98)	0.07	0.04
Erosion basin	Heo and Kwak [3] (HK22)	−0.04	0.37
	Sun et al. [10] (SEA08)	0.27	0.45
	Kim [6] (K98)	0.21	0.39

Within the delta region, the K98 model exhibited the most favorable performance, demonstrating a μ value near zero. In contrast, the HK22 model predicted higher V_S values, resulting in a negative μ, while the SEA08 model predicted lower V_S values, leading to a positive μ. The σ_{ln} values for all models were relatively low (ranging from 0.04 to 0.05), owing to the limited number of reference data points available in the delta region.

Conversely, within the erosion basin region, the HK22 model displayed superior performance. Its μ value was close to zero, and its σ_{ln} value was the lowest among the three models. The SEA08 and K98 models predicted lower V_S values for the erosion basin regions, consequently yielding positive μ values.

Among the three N-V_S models evaluated, the HK22 model showcased the most impressive performance in the erosion basin regions. This achievement can be attributed to the fact that the HK22 model incorporated data from the general urban area (depicted in Figure 1) during its development. This wide data inclusion likely contributed to its accurate predictions within the erosion basin regions. However, it should be noted that the HK22 model faced challenges in accurately predicting $V_{s,soil}$ for the delta region. The K98 model, developed based on reclaimed layers from Yeongjong Island (as shown in Figure 1), demonstrated strong performance within the Nakdonggang delta area. This success aligns with the area's characteristics, including the presence of thick sedimentary layers and a shallow groundwater table. The SEA08 model exhibited distinct trends in comparison to locally calculated $V_{s,soil}$ values within the Busan region. This discrepancy might stem from the utilization of a different regional dataset during the development of the SEA08 model. Such discrepancies emphasize the significance of considering the geological attributes of a specific region when selecting and applying N-V_S models for accurate predictions.

The study conducted a more in-depth analysis of the performance of the HK22 and K98 models based on the variables of bedrock depth and sedimentary layer thickness. Figure 8 provides a visual representation of the residuals in relation to these variables. In the figure, blue dots represent sites within erosion basins, while red dots represent sites in the delta region. The analysis revealed certain trends in the residuals produced by the two models. Residuals generated by the HK22 model exhibited a negative tendency as the bedrock depth increased. Conversely, residuals from the K98 model were distributed near zero when the bedrock depth was deep. In terms of sedimentary layer thickness, the HK22 model resulted in negative residuals for the delta region, whereas the K98 model yielded residuals close to zero in the same region. These observed trends suggest that, apart from geological attributes, the bedrock depth of a specific site plays a significant role in influencing the residuals. This highlights the complex interplay between geological characteristics and other factors when assessing the performance of N-V_S models.

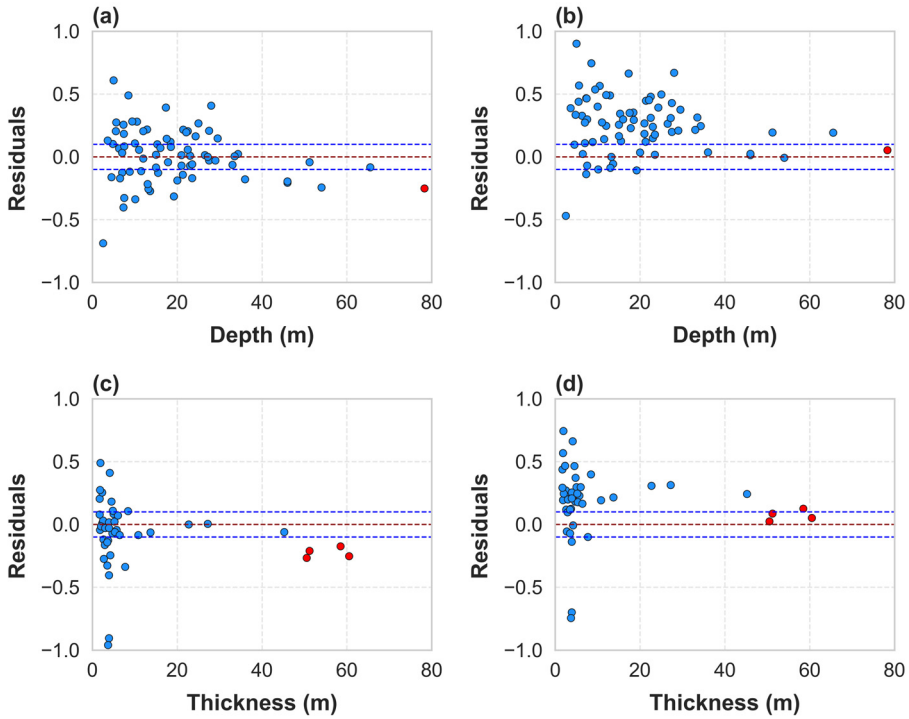


Figure 8. Distribution of residuals versus the bedrock depth for (**a**) HK22 and (**b**) K98 and thickness of sedimentary erosion basin regions for (**c**) HK22 and (**d**) K98.

5. Conclusions

This study conducted an assessment of previously proposed N-V_S relationships by validating the predicted $V_{s,soil}$ values in two distinct geological regions: the Nakdonggang delta and the erosion basin in Busan, South Korea. The results of the analysis revealed the significant impact of geological conditions on the performance of N-V_S relationships. The main findings of this study are summarized as follows:

1. International N-V_S models tend to exhibit consistent trends when the geological attributes of the dataset used for model developments are similar. This pattern was observed in cases of deep sedimentary basins including Kim [6] and Chae [1] in South Korea, Rao and Choudhury [9] in India, and Imai and Tonouchi [4] and Ohsaki and Iwasaki [7] in Japan;
2. Through residual analyses, comparisons were made between $V_{s,soil}$ values derived from field-measured V_S and those calculated using N-V_S models by Kim [6], Sun et al. [10], and Heo and Kwak [3]. These analyses were conducted separately for the Nakdonggang delta and erosion basin regions. The model developed for reclamation land [6] exhibited satisfactory performance for the delta region. Conversely, the model based on locally sourced data [3] performed well in the erosion basin regions. Residual analyses were conducted, comparing field-measured $V_{s,soil}$ values with those calculated using N-V_S models developed by Kim, Sun et al., and Heo and Kwak. These analyses were performed separately for the Nakdonggang delta and erosion basin regions. The model developed for reclamation land showed satisfactory performance for the delta region, while the model based on data primarily from the urban area demonstrated good performance in the erosion basin regions;
3. In the erosion basin region, a more detailed analysis of the residuals predicted by Heo and Kwak [3] and Kim [6] was conducted, focusing on factors like bedrock depth and sedimentary layer thickness. The presence of negative residuals in areas with deep bedrock depths, similar to the delta region, indicates that geological conditions significantly influence the performance of N-V_S relationships.

These findings emphasize the importance of considering the geological context and terrain characteristics when assessing and refining N-V_S relationships for predicting V_S in different regions. The validated N-V_S models presented in this study, tailored to specific geological conditions, can prove valuable in scenarios requiring accurate V_S estimations, such as liquefaction assessments using V_S values [35–42].

Author Contributions: Conceptualization, G.H., J.K., S.J. and D.K.; methodology, G.H. and D.K.; formal analysis, G.H.; investigation, G.H. and J.K.; resources, S.J. and D.K.; data curation, G.H. and J.K.; writing—original draft preparation, G.H.; writing—review and editing, J.K., S.J. and D.K.; visualization, G.H.; supervision, D.K.; project administration, D.K.; funding acquisition, D.K. All authors have read and agreed to the published version of the manuscript.

Funding: This work was supported by the Ministry of Land, Infrastructure and Transport (MLIT) with the grant number RS-2022-00143584.

Data Availability Statement: The data presented in this study are available on request from the corresponding author.

Acknowledgments: We are grateful to MLIT for operating and maintaining the GeoInfo geotechnical database.

Conflicts of Interest: The authors declare no conflict of interest. The funders had no role in the design of the study; in the collection, analyses, or interpretation of data; in the writing of the manuscript; or in the decision to publish the results.

References

1. Chae, H.Y. Evaluation of Saemangeum Dreged Solil by Shear Wave Velocity in the Geophysical Logging. Ph.D. Thesis, Hanyang University, Seoul, Republic of Koea, 2014.
2. Do, J.; Hwang, P.; Chung, S.; Chun, B. Analysis on Relation of S-wave Velocity and N Value for Stratums in Chungcheong Buk-do. *J. Korean GEO-Environ. Soc.* **2011**, *12*, 13–22.
3. Heo, G.S.; Kwak, D.Y. Vs Prediction Model Using SPT-N Values and Soil Layers in South Korea. *J. Korean Geotech. Soc.* **2022**, *38*, 53–66.
4. Imai, T.; Tonoughi, K. Correlation of N value with S-wave velocity and shear modulus. In *Penetration Testing, Volume 1*; Routledge: Oxfordshire, UK, 2021; pp. 67–72.
5. Imai, T.; Yoshimura, Y. Elastic wave velocity and soil properties in soft soil. *Tsuchito-Kiso* **1970**, *18*, 17–22.
6. Kim, D.S. *Development of Quality Evaluation Technique of Ground Improvement on Sands Using SASW Method*; Ministry of Land, Infrastructure and Transport: Sejong-Si, Republic of Koea, 1998.
7. Ohsaki, Y.; Iwasaki, R. On dynamic shear moduli and Poisson's ratios of soil deposits. *Soils Found.* **1973**, *13*, 61–73. [CrossRef]
8. Ohta, Y.; Goto, N. Empirical shear wave velocity equations in terms of characteristic soil indexes. *Earthq. Eng. Struct. Dyn.* **1978**, *6*, 167–187. [CrossRef]
9. Rao, V.D.; Choudhury, D. Estimation of shear wave velocity and seismic site characterization for new nuclear power plant region, India. *Nat. Hazards Rev.* **2020**, *21*, 06020004. [CrossRef]
10. Sun, C.-G.; Kim, H.-J.; Chung, C.-K. Deduction of correlations between shear wave velocity and geotechnical in-situ penetration test data. *J. Earthq. Eng. Soc. Korea* **2008**, *12*, 1–10.
11. Akkaya, İ.; Özvan, A.; Özvan, E.E. A new empirical correlation between pressuremeter modules (EM) and shear wave velocity (Vs) for clay soils. *J. Appl. Geophys.* **2019**, *171*, 103865. [CrossRef]
12. Hasancebi, N.; Ulusay, R. Empirical correlations between shear wave velocity and penetration resistance for ground shaking assessments. *Bull. Eng. Geol. Environ.* **2007**, *66*, 203–213. [CrossRef]
13. Pitilakis, K.; Raptakis, D.; Lontzetidis, K.; Tika-Vassilikou, T.; Jongmans, D. Geotechnical and geophysical description of EURO-SEISTEST, using field, laboratory tests and moderate strong motion recordings. *J. Earthq. Eng.* **1999**, *3*, 381–409. [CrossRef]
14. Uma Maheswari, R.; Boominathan, A.; Dodagoudar, G. Use of surface waves in statistical correlations of shear wave velocity and penetration resistance of Chennai soils. *Geotech. Geol. Eng.* **2010**, *28*, 119–137. [CrossRef]
15. Brandenberg, S.J.; Bellana, N.; Shantz, T. Shear wave velocity as function of standard penetration test resistance and vertical effective stress at California bridge sites. *Soil Dyn. Earthq. Eng.* **2010**, *30*, 1026–1035. [CrossRef]
16. Kwak, D.Y.; Brandenberg, S.J.; Mikami, A.; Stewart, J.P. Prediction equations for estimating shear-wave velocity from combined geotechnical and geomorphic indexes based on Japanese data set. *Bull. Seismol. Soc. Am.* **2015**, *105*, 1919–1930. [CrossRef]
17. Rahimi, S.; Wood, C.M.; Wotherspoon, L.M. Influence of soil aging on SPT-Vs correlation and seismic site classification. *Eng. Geol.* **2020**, *272*, 105653. [CrossRef]
18. Piratheepan, P. Estimating Shear-Wave Velocity from SPT and CPT Data. Master's Thesis, Clemson University, Clemson, SC, USA, 2002.

19. Dikmen, Ü. Statistical correlations of shear wave velocity and penetration resistance for soils. *J. Geophys. Eng.* **2009**, *6*, 61–72. [CrossRef]
20. Jeong, E. *Evolution Study of Sedimentary Environments of Late Pleistocene Caused by Sea-Level Changes in the Nakdong River Estuary, Korea*; Kangwon National University: Chuncheon, Republic of Korea, 2017.
21. Yoon, H.S.; Yoo, C.-I.; Kang, Y.-K.; Ryu, C.-R. Delta development in the Nakdong river estuary: A literature survey. *J. Ocean Eng. Technol.* **2007**, *21*, 22–34.
22. Lee, S.; Yang, M.; Lee, C. Time series analysis of area of deltaic barrier island in Nakdong River using Landsat satellite image. *J. Korean Soc. Surv. Geod. Photogramm. Cartogr.* **2016**, *34*, 457–469. [CrossRef]
23. Chang, C.H. A study on shapes and genetic process of erosion basins. *J. Photo Geogr.* **1997**, *6*, 1–16.
24. Lee, G.R. Formation Ages of Alluvial Fans in Granite Erosional Basins, South Korea. *J. Korean Geomorphol. Assoc.* **2022**, *29*, 21–34. [CrossRef]
25. Lee, G.R.; Park, C.S.; Kim, J.Y.; Lee, H.B.; Jeong, J.-Y. Analysis on Surface Relief of Granitic Erosional Basin in the Middle Part of the Korean Peninsula—A Case Study on the Chuncheon, Wonju, Yeongju and Boeun Basins–. *J. Korean Geomorphol. Assoc.* **2022**, *29*, 1–12.
26. Youn, I.H. The Geomorphic Characteristics of Okcheon Basin & Jincheon Basin. *J. Korean Assoc. Reg. Geogr.* **2001**, *7*, 93–104.
27. Hwang, S.I. The Geomorphic development of alluvial fans in Cheongdo basin, Gyeongsangbuk-do (Province), South Korea. *J. Korean Geogr. Soc.* **2004**, *39*, 514–527.
28. Bull, W.B. The alluvial-fan environment. *Prog. Phys. Geogr.* **1977**, *1*, 222–270. [CrossRef]
29. Yoon, S.O.; Saito, K.; Hwang, S.I.; Oguchi, T.; Tanaka, Y. Morphometric Characteristics of Alluvial Fans in South Korea and Comparisons with those of Japan, Taiwan and the Philippines. *J. Korean Geogr. Soc.* **2010**, *45*, 431–443.
30. Yoon, S.O.; Saito, K.; Hwang, S.I.; Tanaka, Y.; Oguchi, T. The theoretical study and distributional characteristics of alluvial fans in Korean Peninsula. *J. Korean Geogr. Soc.* **2005**, *40*, 335–352.
31. Oguchi, T.; Saito, K.; Kadomura, H.; Grossman, M. Fluvial geomorphology and paleohydrology in Japan. *Geomorphology* **2001**, *39*, 3–19. [CrossRef]
32. Yoshikawa, T. Denudation and tectonic movement in contemporary Japan. *Bull. Dep. Geogr. Univ. Tokyo* **1974**, *6*, 1–14.
33. Choi, I.H.; Kwak, D.Y. Comparison of Methods Predicting Vs30 from Shallow Vs Profiles and Suggestion of Optimized Coefficients. *J. Korean Geotech. Soc.* **2020**, *36*, 15–23.
34. Kim, J.; Heo, G.; Kwak, D.; Jeong, S. The Relationship between Bedrock Depth and Site Fundamental Frequency in the Nakdonggang Delta Region, South Korea. *Geotechnics* **2023**, *3*, 550–560. [CrossRef]
35. Andrus, R.D.; Stokoe II, K.H. Liquefaction resistance of soils from shear-wave velocity. *J. Geotech. Geoenviron. Eng.* **2000**, *126*, 1015–1025. [CrossRef]
36. Andrus, R.D.; Piratheepan, P.; Ellis, B.S.; Zhang, J.; Juang, C.H. Comparing liquefaction evaluation methods using penetration-Vs relationships. *Soil Dyn. Earthq. Eng.* **2004**, *24*, 713–721. [CrossRef]
37. Aytaş, Z.; Alpaslan, N.; Özçep, F. Evaluation of liquefaction potential by standard penetration test and shear wave velocity methods: A case study. *Nat. Hazards* **2023**, *118*, 2377–2417. [CrossRef]
38. Ji, Y.; Kim, B.; Kim, K. Evaluation of liquefaction potentials based on shear wave velocities in Pohang City, South Korea. *Int. J. Geo-Eng.* **2021**, *12*, 3. [CrossRef]
39. Johari, A.; Khodaparast, A.; Javadi, A. An analytical approach to probabilistic modeling of liquefaction based on shear wave velocity. *Iran. J. Sci. Technol. Trans. Civ. Eng.* **2019**, *43*, 263–275. [CrossRef]
40. Kayabali, K. Soil liquefaction evaluation using shear wave velocity. *Eng. Geol.* **1996**, *44*, 121–127. [CrossRef]
41. Oshnavieh, D.; Bagherzadeh Khalkhali, A. Use of shear wave velocity in evaluation of soil layer's condition after liquefaction. *J. Civ. Eng. Mater. Appl.* **2019**, *3*, 119–135.
42. Ulmer, K.J.; Green, R.A.; Rodriguez-Marek, A. A consistent correlation between Vs, SPT, and CPT metrics for use in liquefaction evaluation procedures. In Proceedings of the Geo-Congress 2020, Minneapolis, MN, USA, 25–28 February 2020; pp. 132–140.

Disclaimer/Publisher's Note: The statements, opinions and data contained in all publications are solely those of the individual author(s) and contributor(s) and not of MDPI and/or the editor(s). MDPI and/or the editor(s) disclaim responsibility for any injury to people or property resulting from any ideas, methods, instructions or products referred to in the content.